Biochemistry and Biophysics Reports 3 (2015) 83–93

Contents lists available at ScienceDirect

Biochemistry and Biophysics Reports

journal homepage: www.elsevier.com/locate/bbrep

The histone deacetylase inhibitor cambinol prevents acidic pH_e-induced anterograde lysosome trafficking independently of sirtuin activity

Samantha S. Dykes [a,c], Ellen Friday [b,c], Kevin Pruitt [c,d,1], James A. Cardelli [a,c,*]

[a] Department of Microbiology and Immunology, Louisiana State University Health Sciences Center, 1501 Kings Highway, Shreveport, LA 71130, United States
[b] Department of Medicine, Louisiana State University Health Sciences Center, 1501 Kings Highway, Shreveport, LA 7113, United States
[c] Feist-Weiller Cancer Center, Louisiana State University Health Sciences Center, 1501 Kings Highway, Shreveport, LA 71130, United States
[d] Department of Molecular and Cellular Physiology, Louisiana State University Health Sciences Center, 1501 Kings Highway, Shreveport, LA 71130, United States

ARTICLE INFO

Article history:
Received 17 April 2015
Received in revised form
17 July 2015
Accepted 23 July 2015
Available online 26 July 2015

Keywords:
Cambinol
Lysosome trafficking
Troglitazone
Acidic pH_e
Rab7
ERK

ABSTRACT

Common features of the solid tumor microenvironment, such as acidic extracellular pH and growth factors, are known to induce the redistribution of lysosomes from a perinuclear region to a position near the plasma membrane. Lysosome/plasma membrane juxtaposition facilitates invasion by allowing for the release of lysosomal proteases, including cathepsin B, which contribute to matrix degradation. In this study we identified the sirtuin 1/sirtuin 2 (SIRT1/2) inhibitor cambinol acts as a drug that inhibits lysosome redistribution and tumor invasion. Treatment of cells with cambinol resulted in a juxtanuclear lysosome aggregation (JLA) similar to that seen upon treatment with the PPARγ agonist, troglitazone (Tro). Like Tro, cambinol required the activity of ERK1/2 in order to induce this lysosome clustering phenotype. However, cambinol did not require the activity of Rab7, suggesting that this drug causes JLA by a mechanism different from what is known for Tro. Additionally, cambinol-induced JLA was not a result of autophagy induction. Further investigation revealed that cambinol triggered JLA independently of its activity as a SIRT1/2 inhibitor, suggesting that this drug could have effects in addition to SIRT1/2 inhibition that could be developed into a novel anti-cancer therapy.

1. Introduction

Metastatic disease accounts for ~90% of cancer-associated deaths. Invasion through the basement membrane allows tumor cells to access sites beyond the tissue of origin which is a precondition for metastasis. Although there are protease-independent mechanisms of invasion, it is widely accepted that protease activity greatly contributes to the invasive potential of tumor cells [1,2]. Specifically, the release of lysosomal cathepsins and matrix metalloproteinases are thought to contribute to tumor invasion by promoting degradation of the extracellular matrix. Lysosomes are acidic vesicles that normally function as degradative organelles at the endpoint of the endosomal pathway and are rich in hydrolases and proteases, including cathepsins B, D, and L. Several studies have shown that cathepsin expression is enhanced in invasive cancer cells and secreted cathepsin B can be found at sites of invadopodia formation, supporting the notion that release of lysosome proteases promotes an invasive phenotype [3–7].

Lysosomes traffic along microtubules and actin filaments via the activity of ATP-dependent kinesin and dynein motor complexes [8]. The position of lysosomes within cells can be influenced by extracellular stimuli, resulting in anterograde (plus end) or retrograde (minus end) trafficking. Tumor cells with lysosomes positioned closer to the plasma membrane secrete more proteases and are more invasive when compared to cells with lysosomes clustered near the center of the cell over the microtubule organizing center (MTOC) [9–13]. Several stimuli that are commonly found within the extracellular tumor microenvironment, such as growth factors and acidic pH, drive anterograde lysosome

Abbreviations: SIRT, sirtuin; NHE, sodium proton exchanger; Tro, troglitazone; JLA, juxtanuclear lysosome aggregation; EIPA, ethyl-isopropyl amiloride; LAMP-1, lysosome associated membrane protein 1; HDAC, histone deacetylase; pH_e, extracellular pH; MTOC, microtubule organizing center

* Corresponding author at: Department of Microbiology and Immunology, Louisiana State University Health Sciences Center, 1501 Kings Highway, Shreveport, LA 71130, United States.
E-mail address: JCarde@lsuhsc.edu (J.A. Cardelli).
[1] Present address: Department of Immunology and Molecular Microbiology, Texas Tech University Health Sciences Center, 3601 4th Street, Lubbock, TX 79430, United States.

http://dx.doi.org/10.1016/j.bbrep.2015.07.015

movement, which is critical for invasion [12–14]. In solid tumors, the extracellular pH (pH_e) can reach as low as 6.0 as a result of reduced blood flow, enhanced sodium hydrogen exchanger (NHE) activity, and anaerobic glycolysis (Warburg Effect) [15]. The acidic pH_e has been shown to enhance tumor invasiveness both *in vitro* and *in vivo* [16,17]. Acidic pH_e also stimulates anterograde lysosome trafficking and previous studies have found that this lysosome redistribution is necessary for cathepsin B release and tumor cell invasion in response to acidic pH_e, which is mediated by NHE activity [12]. We previously identified troglitazone (Tro), an antidiabetic PPARγ agonist, and ethyl-isopropyl amiloride (EIPA), an NHE antagonist, as novel inhibitors of anterograde lysosome trafficking. Tro treatment induces a juxtanuclear lysosome aggregation (JLA) in an ERK/Rab7/RILP-dependent manner and inhibits acidic pH_e and growth factor-mediated tumor invasion [10].

Previous studies strongly suggest that inhibition of anterograde lysosome trafficking and protease release could be therapeutically beneficial to slow tumor invasion [10–13]. Due to clinical toxicity associated with Tro treatment, we have begun to use a high-content imaging approach to screen for compounds that also prevent anterograde lysosome trafficking (manuscript in preparation). Our collaborators previously characterized Sirtuin 1 (SIRT1), one of seven class III histone deacetylase (HDAC), as a major contributor to cancer cell migration and invasion [18,19]. Sirtuins are NAD+ dependent deacetylases, are the mammalian homologs of yeast SIR2 (silent information regulator 2), and have many histone and non-histone targets [20]. As sirtuins are often upregulated in cancer, a number of inhibitors have been generated to facilitate the study of the role of individual sirtuins in disease. Cambinol is a β-naphthol compound that is thought to specifically inhibit the deacetylase activity of SIRT1/2. It is well tolerated in mice and has potent antitumor activity *in vivo* [21]. To assess the role of SIRT1/2 activity in cancer cell lines, our collaborators performed a microarray analysis to characterize the gene expression changes between control-treated and cambinol-treated cells (unpublished data) and found that Rab7 mRNA was overexpressed in cambinol treated cells. Rab7 is a small GTPase that specifically localizes to lysosomes, recruits dynein motors to lysosomes *via* its effector RILP, and drives JLA, resulting in decreased tumor invasion [11,22].

The upregulation of Rab7 in response to cambinol treatment suggests that sirtuins may play a role in lysosome trafficking. The goal of this study was to determine the effects of cambinol treatment on lysosome positioning. We found that cambinol was a potent inhibitor of acidic pH_e-mediated anterograde lysosome trafficking. In addition, we showed that the JLA phenotype occurs independently of Rab7 or changes in gene expression, highlighting the distinct differences in mechanism of action compared to Tro. Additionally, we found that cambinol induces JLA independently of its activity as a SIRT1/2 inhibitor, suggesting that cambinol may have effects on other cellular targets. The ability to alter lysosmal trafficking makes cambinol a viable therapeutic agent for slowing tumor progression.

2. Materials and methods

2.1. Cell culture

The human prostate cancer cell lines DU145 ATCC (Manassas, Va) and PPC1 (a generous gift from Dr. Brianna Williams, LSU-Health Shreveport, originally obtained from Brothman [23]) were maintained in RPMI 1604 with 10% FBS and 1% Penicillin–Streptomycin. The human glioma cell line A127 (ATCC) was maintained in DMEM with 10% FBS and 1% Penicillin–Streptomycin. All cells were cultured at 37 °C and 5% CO_2 and passaged upon reaching 80% confluence. For experiments involving treatment with acidic media, cells were treated with RPMI 1604 containing 130 mM NaCl and 10 mM $NaHCO_3$+2% FBS. The pH was adjusted to 6.4 prior to the start of the experiment. SIRT1 and NonTarget shRNA expressing cells were maintained under 3.6 μg/mL Puromycin (Fisher, Waltham, MA).

2.2. Reagents and antibodies

Cambinol, Actinomycin D, TSA, Rapamycin, and Nicotinamide were purchased from Sigma (St. Louis, MO). AK1 and AGK2 were purchased from ChemBridge (San Diego, Ca). EX527 was supplied by Selleck Chemicals (Houston, TX). UO126 was purchased from Calbiochem (Billerica, MA) and used at 10 μM. LAMP-1 antibody (h4A3) was obtained from the Developmental Studies Hybridoma Bank at the University of Iowa and used at a 1:200 dilution. GM130 and EEA1 antibodies (BD Biosciences, San Jose, CA) were used at 1:50. Mitotracker Red (Molecular Probes, Carlsbad, CA) was used according to the manufacturer's protocol. The SIRT1 (B-10) and Ac-tubulin antibodies were purchased from Santa Cruz Biotechnology (Dallas, TX) and was used at 1:1000. pMEK1/2 S271/221, p70 S6 Kinase Thr389, pErk1/2 T202/Y204, Ac-p53 Lys382, LC3I/II, and total Erk1/2 antibodies (Cell Signaling Technology, Beverly, MA) were used at 1:1000 for western blot. Anti-tubulin antibody (NeoMarkers, Fremont, CA) was used at 1:100 for immunofluorescence (IF) and 1:20,000 for western blot analysis. Secondary antibodies include Dylight 594 donkey anti-mouse 1:100 (Jackson IR, West Grove, PA) for immunoflorescence, and HRP-conjugated anti-mouse and anti-rabbit for western blot (GE Healthcare, Pittsburgh, PA) used at 1:5000. Phalloidin 488 (Invitrogen, Carlsbad, CA) was used at 1:200.

2.3. Immunofluorescence

Cells were seeded at 50% confluence on 22 mm coverslips in 6-well dishes. Following experimental treatment, cells were fixed in 4% PFA (pH 7.2) for 20 min at room temperature. Cells were then washed once with Phosphate Buffered Saline (PBS) (Corning, Manassas, VA) and then incubated with primary antibody for one hour at room temperature in BSP (0.25% bovine serum albumin and 0.1% Sapponin in PBS). Cells were washed twice with PBS then incubated for 1 h with secondary antibody in BSP for one hour at room temperature, protected from light. Cells were washed once with PBS, and then incubated with phalloidin in BSP for 20 min at room temperature protected from light. Cells were washed three times with PBS and coverslips were mounted using DAPI with SlowFade gold anti-fade reagent (Invitrogen). For LC3-GFP-mCherry IF, cells were fixed for 7 min in ice-cold methanol, washed with PBS, and coverslips were mounted using DAPI with slow fade gold reagent. Images were taken on a 40× (Olympus UPlanFl 40×/0.75) or 60× (UPlan Apo 60×/0.90) objective using an Olympus BX50 microscope, Roper Scientific Sensys Camera, and MetaView software. Images were pseudocolored and merged using ImageJ.

2.4. Western blot analysis

Cell lysates were harvested in boiling Laemmli buffer containing 2% β-mercaptoethanol and then boiled for five minutes. SDS-PAGE was performed loading equal volume of each sample. Protein was transferred to PVDF membrane, blocked in 5% milk in TBST and incubated with the indicated antibodies overnight at 4 °C. Anti-mouse or anti-rabbit HRP-conjugated secondary antibodies (GE Healthcare) were diluted at 1:5000 in 5% milk TBST. Membrane was developed using Pierce ECL 2 Western Blotting Substrate (Thermo) and Premium Blue X-Ray Film (Phenix). Representative blots are shown.

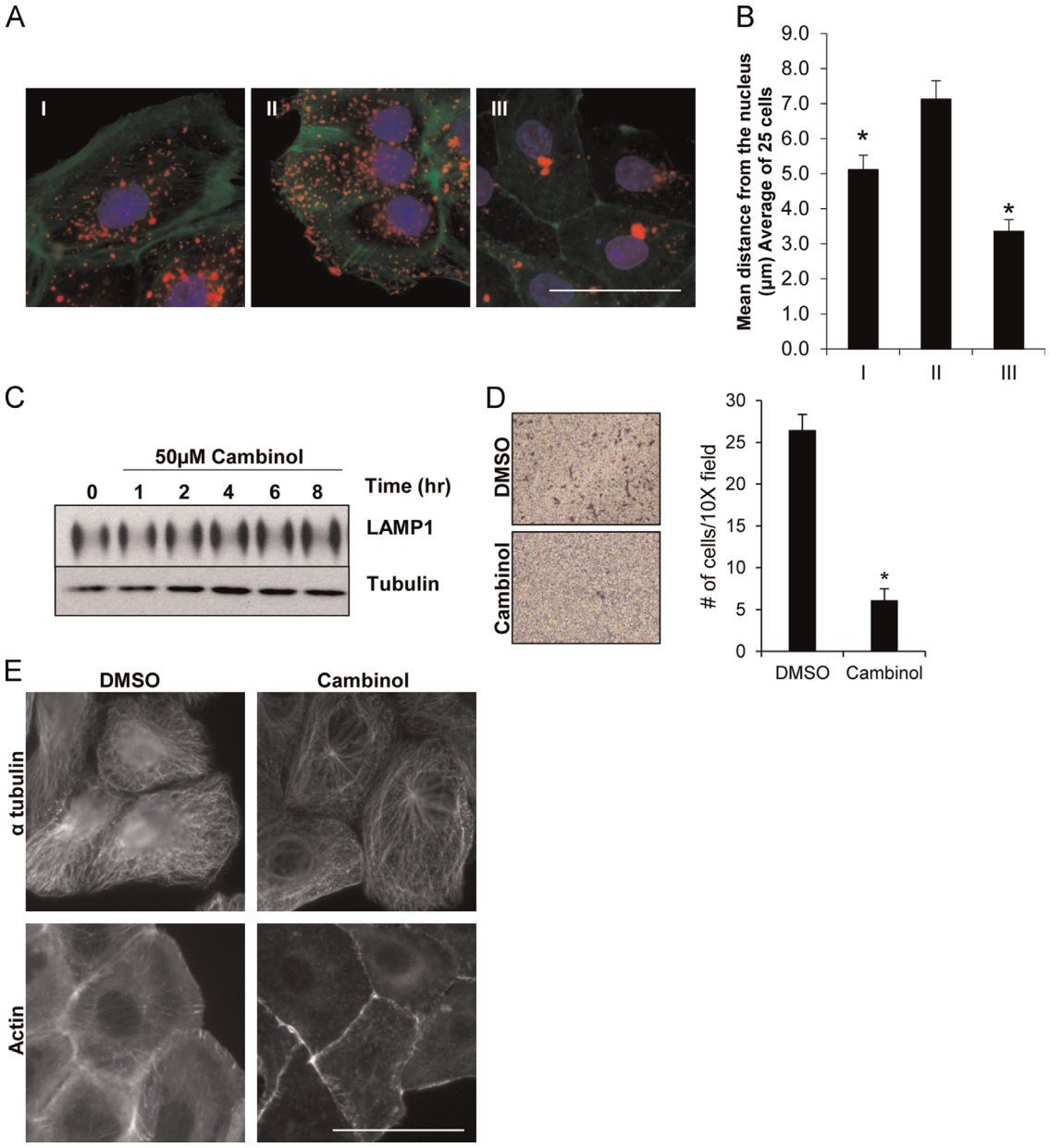

Fig. 1. Cambinol induces juxtanuclear lysosome aggregation and atypical cytoskeleton organization. (A) DU145 prostate cancer cells were treated with (I) vehicle at pH 7.4 for 8 h, (II) vehicle at pH 7.4 for 6 h followed by a 2 h treatment at pH 6.4, or (III) 50 μM cambinol for 6 h in pH7.4 media followed by a 2 h treatment in pH 6.4 media in the continued presence of drug. Cells were stained for LAMP-1 (red), Actin (green), or DAPI (blue) ($N=3$). (B) Represents mean lysosome distribution for 25 cells spanning 3 independent experiments. Error bars represent SEM. $^{*}p < 0.0001$ compared to II. (C) Cells were treated with 50 μM cambinol over time. Whole cell lysates were collected and western blot analysis was performed. (D) DU145 cells were seeded on top of Transwell Inserts coated with a 1:10 dilution of Matrigel in the presence or absence of 50 μM cambinol. Cells that invaded to the underside of the insert were stained with crystal violet and representative 10 × images are shown. Graph represents quantitation from three independent invasion assays. (E) Cells were treated with vehicle or 50 μM cambinol for 6 h at pH 7.4 followed by a 2 h incubation at pH 6.4 plus drug. Cells were then fixed and stained with anti-tubulin or phalloidin ($N=3$). Scale bar represents 50 μm.

2.5. Transwell invasion assay

Cells were pretreated with pH 6.4 buffered RPMI for 48 h prior to the start of the invasion assay. Transwell inserts (Corning) with an 8 μm pore were coated with 50 μL of a 1:10 dilution of Matrigel (Corning, Corning, NY) in serum free media. Matrigel solidified for 30 min at 37°. 3×10^4 cells were seeded on top of the Matrigel-coated insert in a total volume of 100 μL serum free RPMI pH 6.4. pH 6.4 buffered RPMI supplemented with 10% FBS was added to the underside of the insert, and cells were allowed to invade for 24 h. Inserts were then fixed with 4% PFA for 20 min and stained with 0.1% crystal violet (SigmaAldrich) for 20 min. Cells and Matrigel remaining on the top of the insert were removed using a cotton swab. Cells that had invaded to the underside of the insert were imaged using a 10 × objective. The number of invaded cells from three independent experiments were counted.

2.6. Lentiviral delivery of shRNA and LC3 expression vector

The retroviral-based pBABE-mCherry-EGFP-LC3B was a generous gift from the lab of Dr. Nathan Davis [24] and was originally purchased from Addgene (Cambridge, MA, Plasmid #22418). Mission Lentivral Transduction Particles with SIRT1 (TRCN0000018981), Rab7 (TRCN0000007996), or Non-Target shRNA (SHC202V) were

delivered to DU145 prostate cancer cells according to the manufacturer's protocol (Sigma). Briefly, cells were incubated with 6 μg/mL Polybrene and 10 μL lentivirus for 48 h prior to selection with puromycin. Stable cell lines were maintained under puromycin selection and knockdown was assessed by western blot.

2.7. Cell pH and NHE activity assays

Cells were seeded onto custom designed 30 mm chambers (Bioptechs, Biological Optical Technologies, Butler, PA) equipped with a heating element. Cells were assayed for cytosolic pH using BCECF and ratiometric spectrometry as previously described [25]. NHE activity was assayed by incubation in KHH media (140 mM NaCl, 3 mM KCl, 1 mM MgCl, 1 mM $CaCl_2$ and 20 mM HEPES plus 10 mM glucose, pH 7.4) followed by a 4-min NH_4Cl load (KHH in which 20 mM NaCl is replaced with 20 mM NH_4Cl). This was followed by a 1 min exposure to minus sodium (choline chloride substituted for NaCl) after which the pH_i response was continuously monitored for 8 min. After each experiment, the high K^+/nigericin technique was used to clamp the pH_i to media standards of known pH in order to obtain a pH calibration. NHE activity was obtained from the slope of the rapid recovery over the first 30 s and expressed in DpHi/Dtime.

2.8. Lysosome analysis

Analysis of lysosome positioning relative to the nucleus border was achieved using the LysoTracker software, a generous gift from Meiyappan Solaiyappan at Johns Hopkins University. Twenty-five representative cells from three independent experiments were analyzed for each experimental condition. Error bars represent SEM. Significance was determined using Two-Tailed Mann–-Whitney *t* test in GraphPad Software, Prism 3.0.

3. Results

3.1. Cambinol prevents acidic pH_e-induced anterograde lysosome trafficking

We previously reported that acidic pH_e drives anterograde lysosome trafficking and that certain drugs induce JLA that inhibits tumor cell invasion [10–13]. Some of these drugs were shown to activate Rab7. Our collaborators have shown that cells treated with the SIRT1/2 inhibitor, cambinol, exhibited increased Rab7 mRNA expression (unpublished microarray data). Because Rab7 is involved in altering lysosome positioning, we investigated whether cambinol treatment modulated the position of lysosomes within tumor cells. DU145 prostate cancer cells were pretreated with vehicle or cambinol for six hours at pH 7.4 followed by exposure to acidic media (pH 6.4) for two hours in the continued presence of vehicle or drug. Treatment with acidic media serves to drive anterograde lysosome trafficking [12]. Lysosomes were visualized by immunofluorescence microscopy of Lysosome Associated Membrane Protein-1 (LAMP-1) (Fig. 1A). Quantitation of LAMP-1 positive vesicles (red) revealed that acidic pH_e caused a peripheral lysosome distribution relative to neutral pH (compare Fig. 1AI and AII) and that cambinol-treated cells displayed significant JLA when compared to cells treated with acidic media alone (compare Fig. 1 AII with Fig. 1 AIII; quantitated in Fig. 1B). Similar results were observed in the glioma cell line A172 and the prostate cancer cell line PPC1 where cambinol treatment caused JLA (Fig. S1A). Additionally, we treated DU145 (Fig. 1C), PPC1, and A172 cells (Fig. S1B) with cambinol over time and probed for levels of LAMP-1 protein by western blot. We found no change in total LAMP-1 levels upon cambinol treatment, supporting the hypothesis that cambinol is causing lysosome aggregation, rather than exocytosis, resulting in a loss of LAMP-1. Collectively, these data suggest that the effects of cambinol on lysosome distribution are not cell line or tissue-type specific and is not the result of rapid lysosome exocytosis. Furthermore, we pre-treated DU145 cells with pH 6.4 media for 48 h prior to the addition of cambinol and found that cambinol treatment reverses acidic pH_e-mediated anterograde lysosome trafficking (Fig. S1C). Additionally, Transwell invasion assays revealed that cambinol treatment prevented acidic pH_e-mediated invasion of DU145 cells (Fig. 1D), consistent with previous studies showing that inhibition of lysosome trafficking blocks tumor cell invasion [10–13].

Next, we asked whether cambinol treatment caused alteration in the intracellular position of other organelles. DU145 prostate cancer cells were pretreated with vehicle or cambinol for six hours at pH 7.4 followed by exposure to acidic media (pH 6.4) for two hours in the continued presence of vehicle or drug. Cells were then fixed and stained for early endosomes (EEA1), *cis*-Golgi (GM130). Mitochondria were visualized by loading Mitotracker into live cells prior to fixation. Interestingly, cells treated with cambinol also displayed altered distribution of *cis*-Golgi and mitochondria compared to cells exposed to acidic pH_e alone (Fig. S1D). Cambinol treated DU145 prostate cancer cells showed a reduction in the nuclear localized clusters of GM130-positive vesicles (white arrows), and mitochondria appeared disordered, rather than localized in fibrous tracks (white arrows). Although the location of these organelles was not as drastically altered as lysosomes, the disorganized state of *cis*-Golgi and mitochondria in cambinol treated cells suggests that cambinol may be disrupting global organelle trafficking or cytoskeleton dynamics within the cell. To test the possibility of altered cytoskeletal dynamics, we incubated cells with cambinol or vehicle control for six hours at pH 7.4 followed by exposure to acidic media (pH 6.4) for two hours in the presence or absence of cambinol and then stained for α-tubulin or F-actin (Fig. 1E). Vehicle treated cells exhibited robust α-tubulin staining and intense F-actin staining with the appearance of many stress fibers. However, the α-tubulin staining in cells treated with cambinol revealed fewer microtubules, which may indicate reduced microtubule stability. Additionally, cambinol treatment resulted in a loss of stress fibers and an overall reduction in F-actin intensity. These data are consistent with the possibility that cambinol treatment disrupts cytoskeletal dynamics, which may contribute to the altered organelle trafficking.

3.2. Rab7 is not required for cambinol-induced JLA

Previous studies showed that the lysosome localized GTPase Rab7 was necessary for an anti-diabetic agent, Tro, to induce JLA [10,11]. Rab7 is known to engage dynein motors to facilitate inward movement of lysosomes. Due to the association between sirtuin inhibition and upregulation of Rab7 transcript levels (unpublished microarray data), we tested whether Rab7 was also necessary for cambinol mediated JLA. Cells were stably transduced with lentiviral-delivered shRNA to Rab7 and depletion of Rab7 protein compared to NonTarget shRNA cells was confirmed by western blot analysis (Fig. 2A). This level of Rab7 knockdown was sufficient to block Tro-mediated JLA [10,11]. These cells were then treated with cambinol or vehicle for 6 h in pH 7.4 media. Treatment with acidic media was not used because Rab7 expressing cells already have lysosomes localized toward the periphery. Immunofluorescence microscopy to detect LAMP-1 positive vesicles (red) revealed that cambinol induced JLA in both the Non-Target and Rab7 shRNA expressing cells (Fig. 2B and C). These unexpected results demonstrate that Rab7 is not necessary for the JLA induced by cambinol treatment and that cambinol induces JLA by a mechanism different from Tro. Finally, in contrast to microarray data, no increase in Rab7 protein levels was observed in cells treated with cambinol (data not shown), consistent with cambinol altering lysosome positioning independent of Rab7 activity.

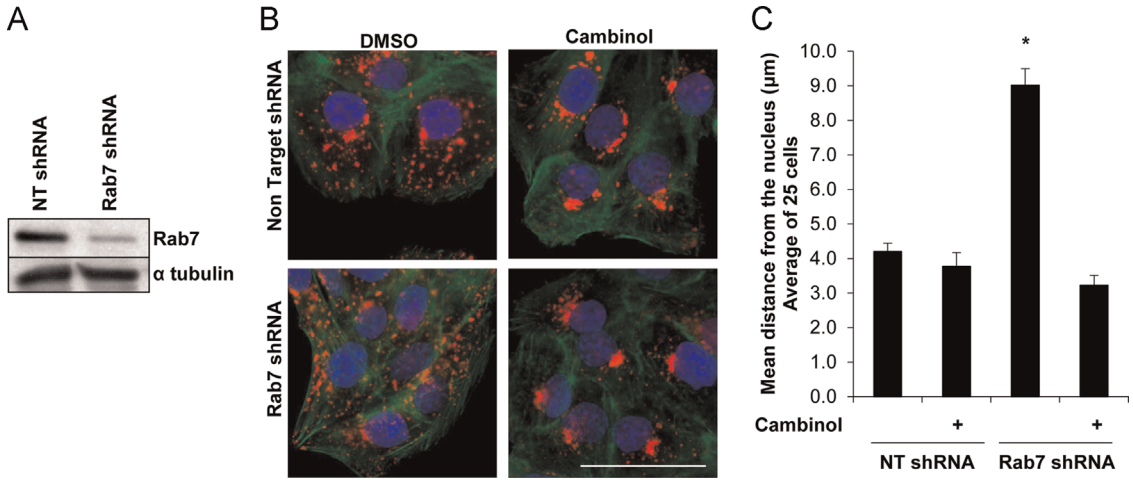

Fig. 2. Cambinol induces juxtanuclear lysosome aggregation independent of Rab7. (A) DU145 prostate cancer cells were transduced with lentiviral delivered shRNA against Rab7. Western blot analysis indicates that Rab7 is depleted. (B) DU145 NonTarget (NT) shRNA expressing cells or Rab7 shRNA expressing cells were treated with vehicle or 50 μM cambinol for 6 h at pH 7.4. Cells were fixed and stained for LAMP-1 (red), phalloidin (green), and DAPI (blue) ($N=3$). Scale bar represents 50 μm. (C) Represents mean lysosome distribution for 25 cells spanning 3 independent experiments. Error bars represent SEM. $^{*}p < 0.0001$ compared to NonTarget DMSO.

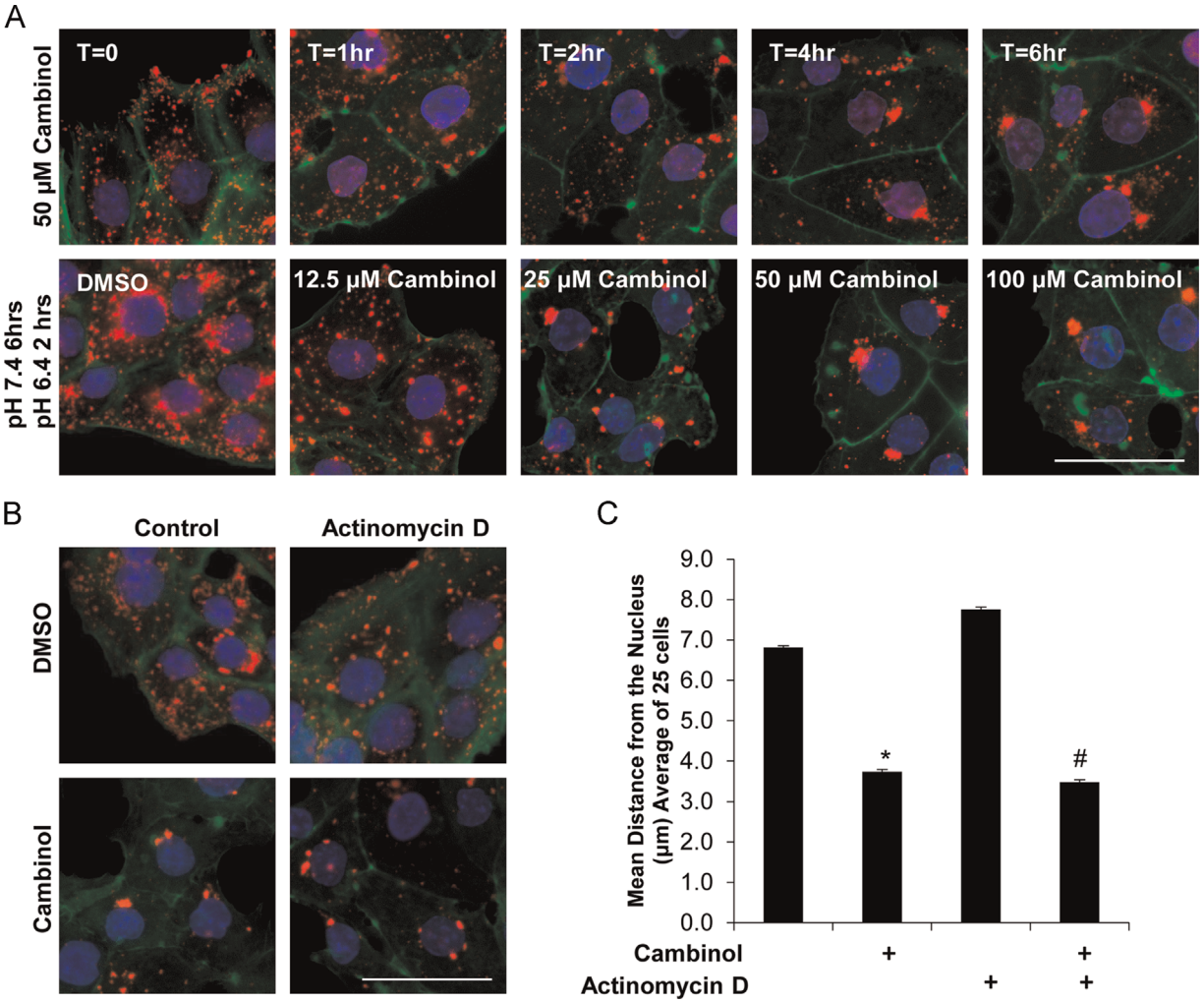

Fig. 3. Cambinol-induced juxtanuclear lysosome aggregation is independent of gene expression changes. (A) DU145 cells were treated with vehicle or 50 μM cambinol for a range of time at pH 7.4 followed by treatment for two hours at pH 6.4 plus drug (top panel). Cells were treated with increasing concentrations of cambinol for 6 h at pH 7.4 followed by 2 h treatment at pH 6.4 plus drug (bottom panel) Cells were fixed and stained with LAMP-1 (red), phalloidin (green), and DAPI (blue) ($N=3$). (B) DU145 were treated with vehicle or 50 μM cambinol in the presence or absence of 10 μM Actinomycin D for 6 h at pH 7.4 followed by a 2 h treatment at pH 6.4 plus drug. Cells were fixed and stained for LAMP-1 (red), phalloidin (green), and DAPI (blue) ($N=3$). Scale bars represent 50 μm. (C) Represents mean lysosome distribution for 25 cells spanning 3 independent experiments. Error bars represent SEM. $^{*}p < 0.0001$ compared to pH 6.4 and $^{\#}p < 0.0001$ compared to Actinomycin D.

3.3. Gene expression changes are not necessary for cambinol-mediated JLA

Tro and the NHE inhibitor EIPA, require a 16 h treatment period before a JLA phenotype is observed [10,13]. This long time frame suggests that changes in gene expression may be necessary for EIPA and Tro to affect lysosome positioning. To test this, DU145 prostate cancer cells were treated with 10 μM Tro in the presence or absence of the mRNA synthesis inhibitor, Actinomycin D (Fig. S2). Tro treatment did not cause JLA in the presence of Actinomycin D, suggesting that changes in gene expression are critical to the mechanism of action of Tro. In order to assess the time frame and minimum concentration of cambinol needed for JLA, DU145 prostate cancer cells were treated with 50 μM cambinol for varying amounts of time (top panel) or varying does of cambinol for 6 h at pH 7.4 followed by a two hour incubation in pH 6.4 media plus drug (bottom panel) (Fig. 3A). We found that cambinol induced JLA in as little as 4 h post-treatment at a concentration of 50 μM and JLA was complete within 8 h of treatment (6 h pH 7.4, 2 h pH 6.4) at concentrations above 25 μM. This short time frame in which cambinol acted suggests that this drug is acting independently of changes in gene expression. Therefore, we then treated cells with cambinol in the presence or absence of Actinomycin D (Fig. 3B and C). Cambinol treatment still resulted in JLA even when transcription was inhibited by Actinomycin D. Taken together, these results supports the hypothesis that unlike Tro, cambinol-induced JLA is independent of gene expression changes.

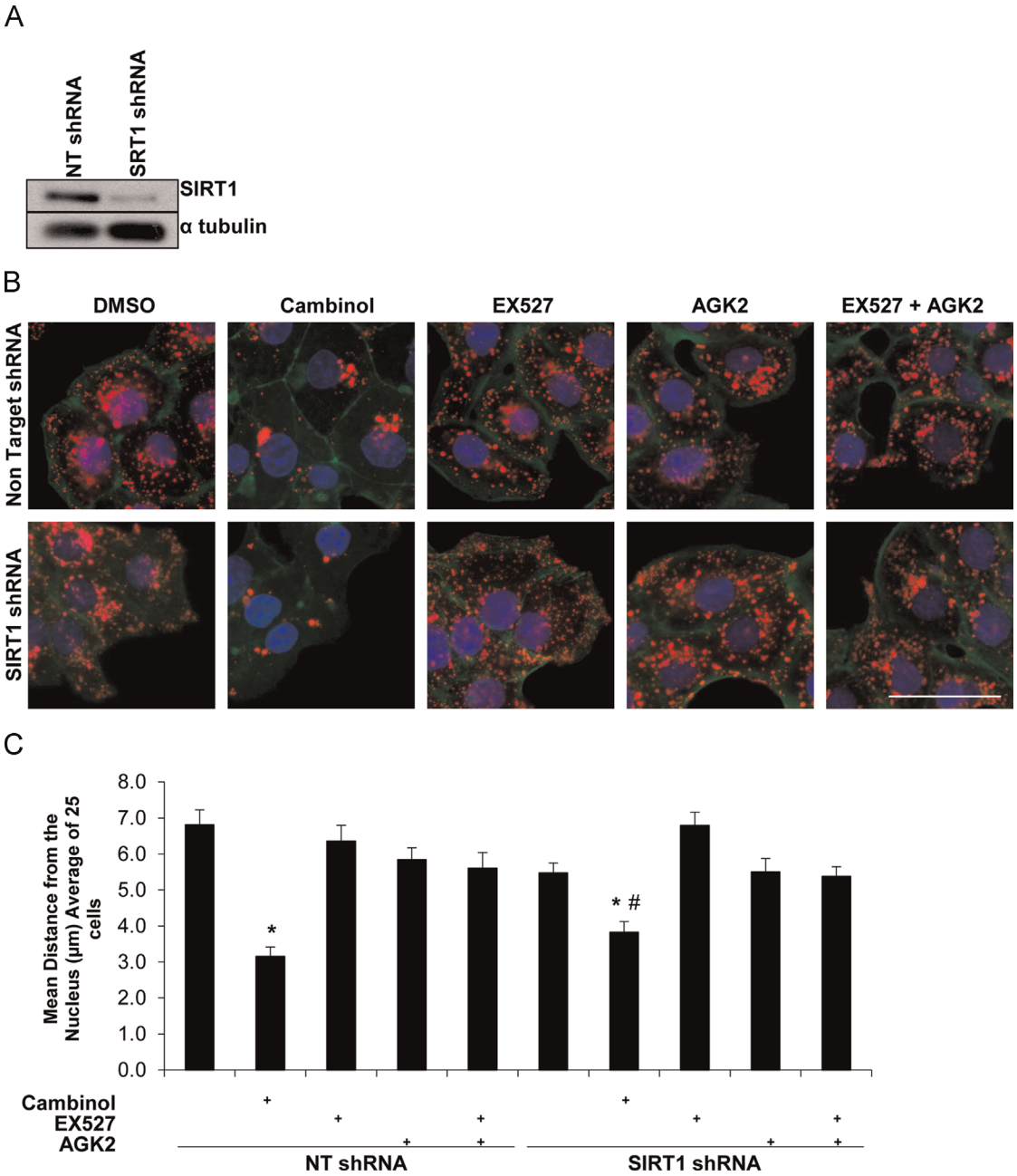

Fig. 4. Cambinol-induced juxtanuclear lysosome aggregation is independent of SIRT1/SIRT2 inhibition. (A) DU145 were transduced with lentiviral delivered shRNA against SIRT1. Western blot analysis indicates that SIRT1 protein levels are reduced in cells expressing SIRT1 shRNA compared to NonTarget shRNA. (B) NonTarget or SIRT1 shRNA expressing DU145 were treated with vehicle or 50 μM cambinol, 3 μM EX527, or 10 μM AGK2 for 6 h in pH 7.4 followed by a 2 h treatment in the presence of drugs at pH 6.4. Cells were fixed and stained for LAMP-1 (red), phalloidin (green), and DAPI (blue) ($N=3$). (C) Represents mean lysosome distribution of 25 cells spanning 3 independent experiments. Error bars represent SEM. $^{*}p < 0.0001$ compared to NT control and $^{\#}p < 0.0004$ compared to SIRT1 KD control.

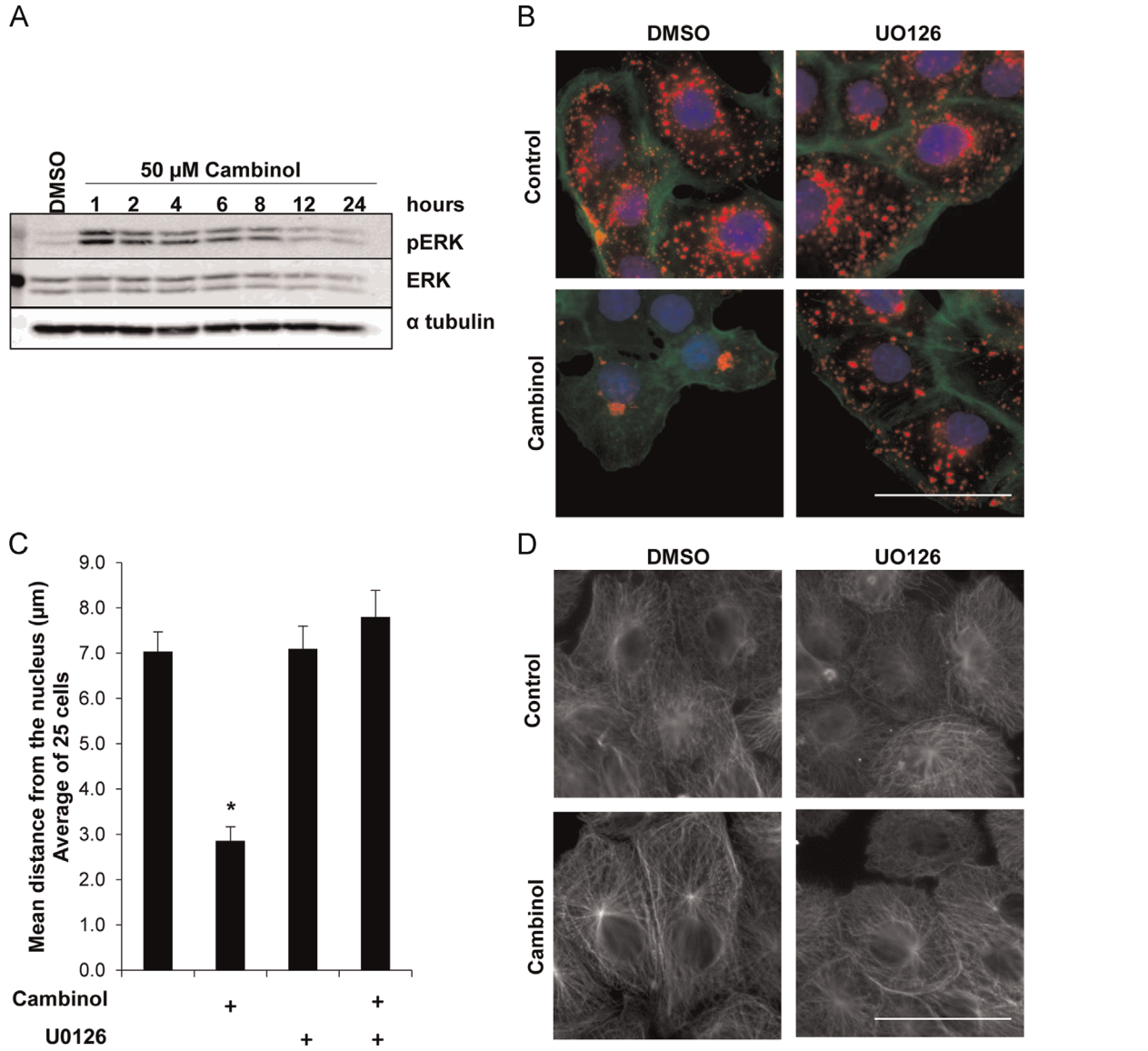

Fig. 5. MAP Kinase signaling is necessary for cambinol-induced juxtanuclear lysosome aggregation. (A) DU145 cells were treated with 50 μM cambinol over time. Whole cell lysates were harvested and levels of total MAPK and activated MAPK were analyzed by western blot ($N=3$). (B) Cells were treated with the MAPK inhibitor, 10 μM UO126, or 50 μM cambinol for 6 h in pH 7.4, followed by a 2 h treatment in pH 6.4 plus drug. Cells were fixed and stained for LAMP-1 (red), phalloidin (green), and DAPI, (blue) ($N=3$). Scale bar represents 50 μm. (C) Represents mean lysosome distribution of 25 cells spanning 3 independent experiments. Error bars represent SEM and $^{*}p > 0.0001$ compared to DMSO control. (D) DU145 cells were treated with the MAPK inhibitor, 10 μM UO126, or 50 μM cambinol for 6 h in pH 7.4, followed by a 2 h treatment in pH 6.4 plus drug. Cells were fixed and stained for α-tubulin ($N=3$). Scale bar represents 50 μm.

3.4. Sirtuins do not regulate lysosome positioning

The significant change in mean lysosome distance from the nucleus observed in cambinol treated cells led us to investigate the mechanism by which this drug causes perinuclear lysosome clustering. We hypothesized that cambinol induced lysosome redistribution by inhibiting SIRT1 or SIRT2 activity, and that the absence of sirtuin activity would result in JLA [21]. To test this hypothesis, we treated DU145 prostate cancer cells with lentiviral-delivered shRNA and depleted SIRT1 protein levels by more than 85% as determined by western blot analysis (Fig. 4A). We then treated SIRT1 knockdown or NonTarget cells with vehicle control for 6 h at pH 7.4 followed by a two hour treatment at pH 6.4. SIRT1 knockdown cells still underwent anterograde lysosome trafficking in response to acidic pH_e similar to NonTarget control cells, suggesting that loss of SIRT1 is not sufficient to prevent acidic pH_e driven lysosome redistribution (Fig. 4B and C). SIRT1 and SIRT2 are reported to have some overlapping targets, most notably, members of the forkhead box O (FOXO) family of transcription factors [26,27]. We were unable to generate KDs of SIRT1 and SIRT2, therefore, we used specific inhibitors that target either SIRT1 (EX527) or SIRT2 (AGK2) [28,29]. The highest non-toxic concentration of inhibitors was used. NonTarget and SIRT1 knockdown cells were treated for 6 h with cambinol, EX527 and AGK2 alone or in combination, or with vehicle control and then exposed to 2 h of acidic pH_e (to induce lysosome movement) in the presence of the specified drug. Cells were fixed and stained for LAMP-1 (red). LAMP-1-positive vesicles were still found to redistribute to the plasma membrane in response to acidic pH_e even in the presence of duel SIRT1 and SIRT2 inhibition (Fig. 4B and C). These data suggest that SIRT1 and/or SIRT2 activity is not necessary for anterograde lysosome trafficking. To investigate the possible role of other HDACs in anterograde lysosome trafficking, we examined lysosomal localization in cells treated with two HDAC inhibitors, nicotinomide and trichostatin A (TSA). Nicotinamide is a byproduct of the NAD^+ dependent-deacetylation reaction and

excess Nicotinamide prevents class III HDAC activity [30,31], while TSA is an inhibitor of class I and class II HDACs [32]. DU145 cells were treated with vehicle, nicotinomide, or TSA for 6 h in pH 7.4 and then moved to acidic media (pH 6.4) containing the same treatment for an additional 2 h. LAMP-1 staining showed that lysosomes in cells treated with nicotinomide or TSA were positioned throughout the cell, similar to vehicle-treated cells (Fig. S3A). As a control to show that these inhibitors were working, DU145 cells were treated with the afore mentioned sirtuin inhibitors and levels of acetylated tubulin (Fig. S3B) or acetylated p53 (Fig. S3C) were detected by western blot. Collectively, these data indicate that cambinol treatment prevents anterograde lysosome trafficking independent of its role as an HDAC inhibitor and that HDAC inhibition alone is not sufficient to drive JLA.

3.5. Cambinol treatment does not inhibit sodium proton exchanger activity

Lysosomes traffic toward the plasma membrane in response to decreased cytosolic pH [12,14]. This cytosolic pH is regulated, in part, by the activity of NHEs. As such, NHE inhibitors reverse anterograde lysosome trafficking. We previously characterized Tro as a potent inhibitor of NHE activity, which in turn drives JLA [10–13]. We wondered whether cambinol, like Tro, also inhibited NHE activity. To test this, NHE activity and cytosolic pH were measured in the presence or absence of cambinol (Fig. S4). Exchanger activity was not decreased in cambinol treated cells compared to control. This indicates that cambinol is not acting as an NHE inhibitor and is in fact causing JLA by a mechanism different from that mediating the effect of Tro.

3.6. ERK1/2 activity is necessary for cambinol-induced JLA

Retrograde lysosomal transport is regulated in part by the ORP1L/RILP/dynein complex, and ERK1/2 plays a role in the assembly of this complex [33]. Tro treatment results in the activation of ERK1/2 signaling, which this is necessary for JLA [10]. To investigate whether cambinol modulates ERK1/2 activity, cells were treated with 50 μM cambinol for different lengths of time spanning 24 h and levels of phosphorylated (active) and total ERK1/2 were determined by western blotting (Fig. 5A). Cambinol treatment induced a robust activation of ERK1/2 at one hour post-treatment, and this activity was sustained until 12 h post-treatment. We found no change in levels of total ERK1/2 protein. Additionally, cambinol treatment caused activation of MEK1/2, the upstream mitogen activated protein kinase that is responsible for ERK1/2 activation (Fig. S5) [34]. To elucidate the role of ERK1/2 activity in cambinol-mediated JLA, cells were treated at pH 7.4 with cambinol in the presence or absence of the ERK1/2 specific inhibitor U0126 for six hours followed by a two hour treatment with acidic pH_e (pH 6.4) plus drug (Fig. 5B). Cells were then fixed, stained with LAMP-1 (red), phalloidin (green) and DAPI (blue) and assessed for lysosome positioning. Control treated cells displayed lysosomes located close to the cell periphery, while cells treated with cambinol alone showed lysosomes clustered near the nucleus. However, cells treated with cambinol in the presence of the ERK1/2 inhibitor U0126 did not show lysosome aggregation and instead had lysosomes diffuse throughout the cell (Fig. 5B and C), suggesting that ERK1/2 activity is necessary for cambinol mediated JLA. Cambinol treatment resulted in reduced cytoskeleton integrity (Fig. 1E), which may partially account for the JLA phenotype. ERK1/2 is known to associate with microtubules and to influence microtubule stability [35]. We asked whether this MAPK pathway regulated cambinol-mediated cytoskeletal changes. To test this, DU145 cells were treated with cambinol or U0126 at pH 7.4 for six hours followed by a two hour treatment with acidic pH_e (pH 6.4) plus drug (Fig. 5D). Immunofluorescence microscopy of α-tubulin revealed that inhibition of ERK1/2 partially prevented cambinol-mediated microtubule loss. Collectively, these data imply that cambinol is disrupting organelle trafficking *via* an ERK1/2-mediated microtubule disruption.

3.7. Cambinol-induced JLA is not a result of autophagy induction

Nutrient starvation can lead to the activation of autophagy, a catabolic process that delivers cytoplasmic contents to the lysosome for degradation (reviewed in [36]). Autophagy is controlled by mammalian target of Rapamycin (mTOR), which inhibits autophagy under permissive growth conditions. The induction of autophagy causes the formation of membrane-bound autophagosomes which fuse with lysosomes in the juxtanuclear region to form autophagolysosomes, leading to an accumulation of these LAMP-1-positive vesicles in the perinuclear space [37]. Autophagy can be regulated by MEK/ERK1/2 signaling [38], and because cambinol requires ERK1/2 activation for JLA (Fig. 5), we investigated whether cambinol treatment activated autophagy. To test whether cambinol influenced the activity of the mTOR pathway, DU145 prostate cancer cells were treated with 50 μM cambinol over an 8 h time course. As a positive control for induction of autophagy cells were treated with Rapamycin for 8 h. Whole cell lysates were collected and probed for phospho-S6 kinase, a mitogen-activated serine/threonine kinase downstream of mTOR, by western blot (Fig. 6A). Rapamycin treatment activated autophagy as indicated by the loss of p70 S6 kinase phosphorylation. However, p70 S6 kinase was not dephosphorylated under conditions of cambinol treatment, suggesting that cambinol does not activate the autophagy pathway *via* mTOR inhibition. Additionally, cambinol treatment did not lead to the appearance of Light Chain 3 II (LC3II) as seen with Rapamycin treatment (Fig. 6B). For further conformation, DU145 prostate cancer cells were generated to stably express GFP and mCherry tagged LC3, a marker of autophagosome and autophagolysosome membranes [39]. Cells were then treated with vehicle, 50 μM cambinol, or 1 μM Rapamycin for 6 h at pH 7.4 followed by a 2 h treatment in pH 6.4 media plus drug. Immunofluorescence microscopy revealed that Rapamycin treatment caused perinuclear aggregation of GFP and mCherry tagged LC3, but vehicle or cambinol treatment did not (Fig. 6C). Collectively, these data imply that cambinol is not activating the autophagy pathway as a mechanism for JLA.

4. Discussion

In the present study we identify cambinol, a sirtuin inhibitor, as a potent regulator of lysosome trafficking and inducer of JLA. Cambinol stimulates JLA independently from Rab7, NHE inhibition or gene expression changes, indicating that cambinol acts to aggregate lysosomes by a mechanism that is highly distinct from that of Tro. Additionally, cambinol does not activate autophagy as a means to drive JLA and sirtuin inhibition alone is not sufficient to drive JLA. We found that cambinol treatment, similar to Tro, does activate ERK, which is required for JLA.

The peripheral trafficking of juxtanuclear localized lysosomes in response to microenvironment stimuli results in the enhanced invasion of tumor cells [10–13]. This anterograde lysosome trafficking movement facilitates the release of lysosomal proteases, such as cathepsin B, which degrade the surrounding matrix allowing for cell invasion. Increased cathepsin B expression is associated with invasive cancers and several studies have shown that inhibiting cathepsin B greatly reduces invasion and metastasis *in vitro* and *in vivo* [3–5,40–42]. Despite the well-characterized role of cathepsins and other proteases such as MMPs in tumor invasion, protease inhibitors have repeatedly failed clinical trials

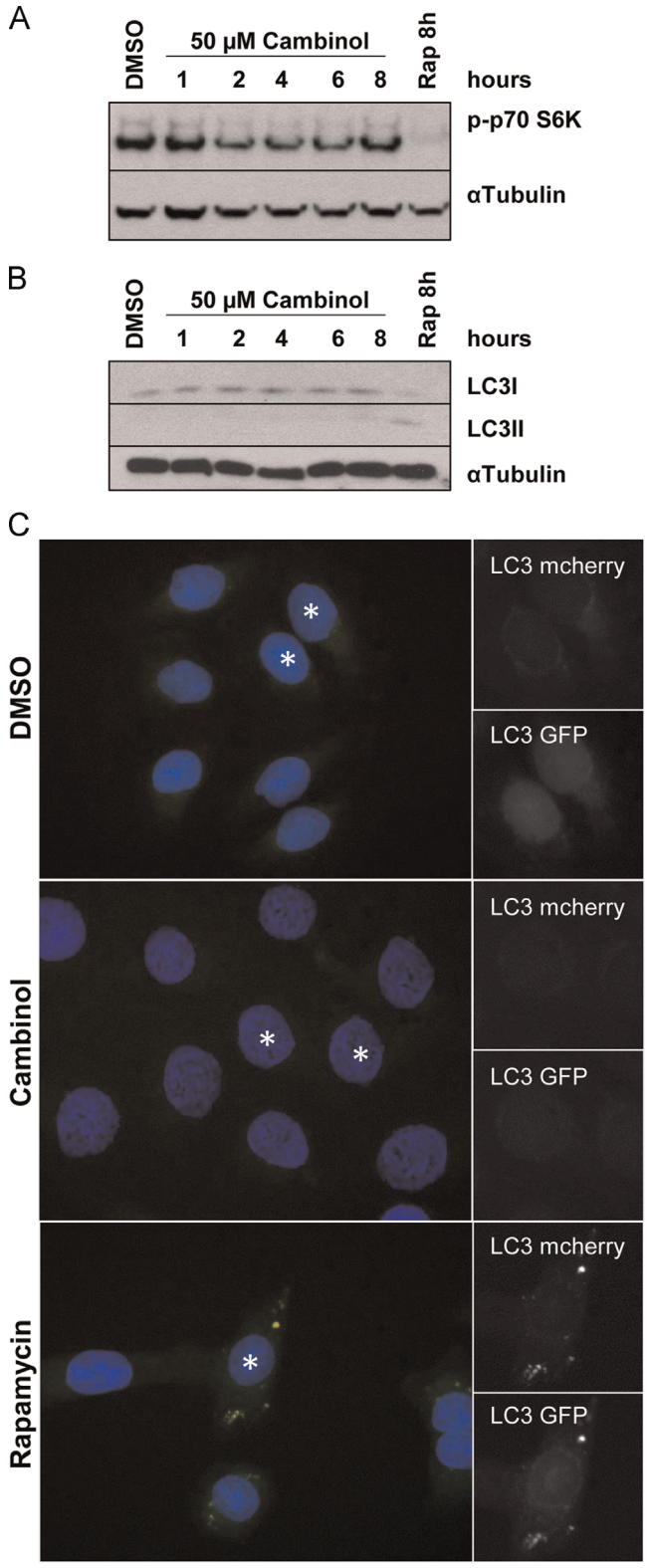

Fig. 6. Cambinol treatment does not induce autophagy. (A) DU145 cells were treated with 50 μM cambinol over time or 1 μM Rapamycin for 8 h. Whole cell lysates were collected and probed for the indicated proteins by western blot ($N=3$). (B) DU145 cells were treated with 50 μM cambinol over time or 1 μM Rapamycin for 8 h. Whole cell lysates were collected and probed for the indicated proteins by western blot. (C) DU145 prostate cells were made to express LC3-GFP-mcherry. Cells were treated with vehicle, 50 μM cambinol, or 1 μM Rapamycin for 6 h in pH 7.4, followed by a 2 h treatment in pH 6.4 plus drug. Cells were fixed in methanol and stained with DAPI. Representative 60X images are shown, $N=3$. * represents cells included in split channel panel.

due to toxicity and poor trial endpoint selection [43]. Therefore, a novel modality of preventing protease release from the cell might prove to be more therapeutically successful. To that end, we are seeking to identify compounds that are novel inhibitors of anterograde lysosome trafficking and predict they will inhibit tumor cell invasion and subsequent metastasis.

We found the sirtuin inhibitor cambinol to be a potent inhibitor of acidic pH_e-stimulated lysosome trafficking and this effect to be independent of Rab7, which is in contrast to Rab7-mediated JLA induced by Tro (Figs. 1 and 2). Our laboratory has previously detailed the ability of Tro to initiate a JLA phenotype in an ERK/Rab7/RILP-dependent manner; however, several reports have demonstrated an unsatisfactory toxicity profile for this agent [10]. A unique mechanism of action to induce JLA may overcome the toxicity reported for Tro. Based on the differences reported here for the time post-treatment required for JLA, and the sensitivity of JLA induction to Actinomycin D treatment, we conclude that the mechanisms of Tro and cambinol are highly distinct.

In addition to their role in histone de-acetylation and control of transcription, SIRT1 and SIRT2 also de-acetylate many non-histone targets. Acetylation of a positively charged lysine can alter protein structure, prevent ubiquitination, and influence affinity to binding partners (reviewed in [44]). It is possible that cambinol treatment influences the acetylation and activity of proteins known to be involved in lysosome movement. Of note, Sirtuins are reported to deacetylate major cytoskeletal components such as tubulin and cortactin, a known regulator of actin polymerization [45,46]. Lysosomes and other organelles are trafficked along microtubules and actin filaments through the action of kinesin and dynein motors, and lysosomes can be found in cortactin-rich invadopodia [6,8]. Interestingly, we did observe that microtubules and F-actin organization was altered in cambinol-treated cells (Fig. 1D). This altered cytoskeletal arrangement may be at least partially responsible for the lysosome clustering seen upon cambinol treatment. However, we found that Sirtuin1 knockdown or pharmacological inhibition of both SIRT1 and SIRT2 did not induce JLA (Fig. 4B and C), suggesting that any organelle trafficking or cytoskeletal defects with cambinol treatment may be independent from its activity as a SIRT1/2 inhibitor. While specific HDACs are known to facilitate organelle trafficking [47], the data presented herein suggest that, in general, HDACs do not play a role in acidic pH_e-mediated lysosome trafficking. We conclude that the JLA seen with cambinol treatment is most likely due to an as-yet unidentified pathway altered by the drug treatment. We are not the first to report that cambinol has 'off target' effects. The Roger lab recently reported that cambinol and sirtinol treatment blocked cytokine production in macrophages independently of SIRT1/2 inhibition [48].

Tro activates the MAPK pathway and ERK 1/2 activation is necessary for Tro-mediated lysosome clustering [10]. Similarly, cambinol also activated ERK 1/2 and this activation is necessary for cambinol-mediated JLA. This finding is in contrast to previous reports from the Roger and Liu lab's that cambinol treatment or SIRT1 inhibition results in decreased ERK1/2 phosphorylation [48,49]. The discrepancies between our findings and previously published results may be explained by varying cell lines and concentrations/timeframes of cambinol treatment. ERK1/2 can localize to and signal from late endosomes and lysosome membranes and lysosome-localized ERK1/2 is thought to aid in the activation and/or recruitment of the Rab7/RILP/Dynein complex [50,51]. However, our data indicates that cambinol can cause JLA independently of Rab7 (Fig. 2), suggesting that ERK1/2-mediated regulation of Rab7/RILP/Dynein is not the mechanism by which cambinol triggers lysosome clustering. Several studies report that ERK1/2 activity is necessary for the formation of mature autophagolysosomes, which are starvation induced LAMP-1 positive

structures commonly found in the perinuclear region [38,52,53]. However, our data suggests that cambinol treatment is not stimulating autophagy (Fig. 6), and that cambinol-induced JLA is not a result of autophagolysosome formation. However, we did find that ERK1/2 inhibition abrogated cambinol's effects on the microtubule network (Fig. 5D). As lysosomes and other organellese traffic along microtubules, this ERK1/2-mediated cytoskeletal disruption is most likely the mechanism by which cambinol induces JLA. The precise molecular mechanisms by which cambinol activates MEK1/2 and ERK1/2 remain to be determined.

Both sirtuins and peripheral lysosome trafficking contribute to tumor progression. Due to drug resistance, multimodality cancer treatments are gaining traction and it may be beneficial to target lysosome trafficking in addition to sirtuin inhibition. Currently there are several HDAC inhibitors in clinical trials as anti-cancer drugs [54]. Although we have shown that cambinol does indeed induce JLA and this drug is reported to inhibit tumor invasion *in vitro* and *in vivo,* cambinol may not be marketable for clinical applications due to these unknown 'off target' properties [21]. Tro also prevents anterograde lysosome trafficking, but Tro and many other thiazolidendione family drugs have been removed from the clinic due to toxicity. Although Tro and cambinol may not be ideal for use in a clinical setting, the study of the mechanisms by which these drugs redistribute lysosomes will contribute to our overall understanding of the molecular mechanisms that govern lysosome trafficking. Therefore, future studies aim to identify the precise mechanism by which cambinol and Tro trigger JLA. Additionally, we plan to investigate novel compounds that prevent anterograde lysosome trafficking, similar to that of Tro and cambinol, and their role in inhibiting tumor invasion. Finally, it would be interesting to test cambinol in combination with other lysosome trafficking inhibitors to determine if it will enhance effectiveness of antitumor therapies.

Conflict of interest

The authors have no conflict of interest to disclose.

Acknowledgments

We would like to thank Adam Greer for assistance with making the LC3-GFP-mcherry expressing DU145 cells. We would also like to acknowledge Meiyappan Solaiyappan (Johns Hopkins) for the lysosome quantification software and Min Chu for technical assistance. Special thanks to Drs. David Coleman and Michelle Arnold for the critical reading of this document. This work was funded by a Carroll Feist Pre-doctoral Fellowship (Grant no. 149741195A) awarded to SSD.

Appendix A. Supplementary material

Supplementary data associated with this article can be found in the online version at http://dx.doi.org/10.1016/j.bbrep.2015.07.015.

References

[1] P. Friedl, K. Wolf, Tube travel: the role of proteases in individual and collective cancer cell invasion, Cancer Res. 68 (2008) 7247–7249.
[2] F. Sabeh, R. Shimizu-Hirota, S.J. Weiss, Protease-dependent versus -independent cancer cell invasion programs: three-dimensional amoeboid movement revisited, J. Cell Biol. 185 (2009) 11–19.
[3] I. Podgorski, B.E. Linebaugh, M. Sameni, C. Jedeszko, S. Bhagat, et al., Bone microenvironment modulates expression and activity of cathepsin B in prostate cancer, Neoplasia 7 (2005) 207–223.
[4] S. Roshy, B.F. Sloane, K. Moin, Pericellular cathepsin B and malignant progression, Cancer Metastasis Rev. 22 (2003) 271–286.
[5] A.A. Sinha, M.J. Wilson, D.F. Gleason, P.K. Reddy, M. Sameni, et al., Immunohistochemical localization of cathepsin B in neoplastic human prostate, Prostate 26 (1995) 171–178.
[6] C. Tu, C.F. Ortega-Cava, G. Chen, N.D. Fernandes, D. Cavallo-Medved, et al., Lysosomal cathepsin B participates in the podosome-mediated extracellular matrix degradation and invasion via secreted lysosomes in v-Src fibroblasts, Cancer Res. 68 (2008) 9147–9156.
[7] T. Kirkegaard, M. Jaattela, Lysosomal involvement in cell death and cancer, Biochim. Biophys. Acta 1793 (2009) 746–754.
[8] M.N. Cordonnier, D. Dauzonne, D. Louvard, E. Coudrier, Actin filaments and myosin I alpha cooperate with microtubules for the movement of lysosomes, Mol. Biol. Cell 12 (2001) 4013–4029.
[9] Y. Liu, Y. Zhou, K. Zhu, Inhibition of glioma cell lysosome exocytosis inhibits glioma invasion, PLoS One 7 (2012) e45910.
[10] J.J. Steffan, J.A. Cardelli, Thiazolidinediones induce Rab7-RILP-MAPK-dependent juxtanuclear lysosome aggregation and reduce tumor cell invasion, Traffic 11 (2010) 274–286.
[11] J.J. Steffan, S.S. Dykes, D.T. Coleman, L.K. Adams, D. Rogers, et al., Supporting a role for the GTPase Rab7 in prostate cancer progression, PLoS One 9 (2014) e87882.
[12] J.J. Steffan, J.L. Snider, O. Skalli, T. Welbourne, J.A. Cardelli, Na^+/H^+ exchangers and RhoA regulate acidic extracellular pH-induced lysosome trafficking in prostate cancer cells, Traffic 10 (2009) 737–753.
[13] J.J. Steffan, B.C. Williams, T. Welbourne, J.A. Cardelli, HGF-induced invasion by prostate tumor cells requires anterograde lysosome trafficking and activity of Na^+–H^+ exchangers, J. Cell Sci. 123 (2010) 1151–1159.
[14] K. Glunde, S.E. Guggino, M. Solaiyappan, A.P. Pathak, Y. Ichikawa, et al., Extracellular acidification alters lysosomal trafficking in human breast cancer cells, Neoplasia 5 (2003) 533–545.
[15] R.J. Gillies, N. Raghunand, G.S. Karczmar, Z.M. Bhujwalla, MRI of the tumor microenvironment, J. Magn. Reson. Imaging 16 (2002) 430–450.
[16] R. Martinez-Zaguilan, E.A. Seftor, R.E. Seftor, Y.W. Chu, R.J. Gillies, et al., Acidic pH enhances the invasive behavior of human melanoma cells, Clin. Exp. Metastasis 14 (1996) 176–186.
[17] E.K. Rofstad, B. Mathiesen, K. Kindem, K. Galappathi, Acidic extracellular pH promotes experimental metastasis of human melanoma cells in athymic nude mice, Cancer Res. 66 (2006) 6699–6707.
[18] K.R. Holloway, T.N. Calhoun, M. Saxena, C.F. Metoyer, E.F. Kandler, et al., SIRT1 regulates Dishevelled proteins and promotes transient and constitutive Wnt signaling, Proc. Natl. Acad. Sci. USA 107 (2010) 9216–9221.
[19] M. Saxena, S.S. Dykes, S. Malyarchuk, A.E. Wang, J.A. Cardelli, et al., The sirtuins promote Dishevelled-1 scaffolding of TIAM1, Rac activation and cell migration, Oncogene 34 (2013) 188–198.
[20] S. Imai, C.M. Armstrong, M. Kaeberlein, L. Guarente, Transcriptional silencing and longevity protein Sir2 is an NAD-dependent histone deacetylase, Nature 403 (2000) 795–800.
[21] B. Heltweg, T. Gatbonton, A.D. Schuler, J. Posakony, H. Li, et al., Antitumor activity of a small-molecule inhibitor of human silent information regulator 2 enzymes, Cancer Res. 66 (2006) 4368–4377.
[22] I. Jordens, M. Fernandez-Borja, M. Marsman, S. Dusseljee, L. Janssen, et al., The Rab7 effector protein RILP controls lysosomal transport by inducing the recruitment of dynein-dynactin motors, Curr. Biol. 11 (2001) 1680–1685.
[23] A.R. Brothman, L.J. Lesho, K.D. Somers, G.L. Wright Jr., D.J. Merchant, Phenotypic and cytogenetic characterization of a cell line derived from primary prostatic carcinoma, Int. J. Cancer 44 (1989) 898–903.
[24] A.H. Greer, T. Yong, K. Fennell, Y.W. Moustafa, M. Fowler, et al., Knockdown of core binding factorbeta alters sphingolipid metabolism, J. Cell. Physiol. 228 (2013) 2350–2364.
[25] T. Welbourne, G. Su, G. Coates, R. Routh, K. McCarthy, et al., Troglitazone induces a cellular acidosis by inhibiting acid extrusion in cultured rat mesangial cells, Am. J. Physiol. Regul. Integr. Comp. Physiol. 282 (2002) R1600–R1607.
[26] D. Frescas, L. Valenti, D. Accili, Nuclear trapping of the forkhead transcription factor FoxO1 via Sirt-dependent deacetylation promotes expression of glucogenetic genes, J. Biol. Chem. 280 (2005) 20589–20595.
[27] F. Wang, M. Nguyen, F.X. Qin, Q. Tong, SIRT2 deacetylates FOXO3a in response to oxidative stress and caloric restriction, Aging Cell 6 (2007) 505–514.
[28] J.M. Solomon, R. Pasupuleti, L. Xu, T. McDonagh, R. Curtis, et al., Inhibition of SIRT1 catalytic activity increases p53 acetylation but does not alter cell survival following DNA damage, Mol. Cell. Biol. 26 (2006) 28–38.
[29] T.F. Outeiro, E. Kontopoulos, S.M. Altmann, I. Kufareva, K.E. Strathearn, et al., Sirtuin 2 inhibitors rescue alpha-synuclein-mediated toxicity in models of Parkinson's disease, Science 317 (2007) 516–519.
[30] K.J. Bitterman, R.M. Anderson, H.Y. Cohen, M. Latorre-Esteves, D.A. Sinclair, Inhibition of silencing and accelerated aging by nicotinamide, a putative negative regulator of yeast sir2 and human SIRT1, J. Biol. Chem. 277 (2002) 45099–45107.
[31] J.L. Avalos, K.M. Bever, C. Wolberger, Mechanism of sirtuin inhibition by nicotinamide: altering the NAD(+) cosubstrate specificity of a Sir2 enzyme, Mol. Cell 17 (2005) 855–868.
[32] M. Yoshida, M. Kijima, M. Akita, T. Beppu, Potent and specific inhibition of mammalian histone deacetylase both in vivo and in vitro by trichostatin A, J. Biol. Chem. 265 (1990) 17174–17179.
[33] M. Johansson, N. Rocha, W. Zwart, I. Jordens, L. Janssen, et al., Activation of endosomal dynein motors by stepwise assembly of Rab7-RILP-p150Glued,

ORP1L, and the receptor betalll spectrin, J. Cell Biol. 176 (2007) 459–471.
[34] C.M. Crews, A. Alessandrini, R.L. Erikson, The primary structure of MEK, a protein kinase that phosphorylates the ERK gene product, Science 258 (1992) 478–480.
[35] R.E. Harrison, E.A. Turley, Active erk regulates microtubule stability in H-ras-transformed cells, Neoplasia 3 (2001) 385–394.
[36] D. Glick, S. Barth, K.F. Macleod, Autophagy: cellular and molecular mechanisms, J. Pathol. 221 (2010) 3–12.
[37] S. Kimura, T. Noda, T. Yoshimori, Dynein-dependent movement of autophagosomes mediates efficient encounters with lysosomes, Cell Struct. Funct. 33 (2008) 109–122.
[38] J. Wang, M.W. Whiteman, H. Lian, G. Wang, A. Singh, et al., A non-canonical MEK/ERK signaling pathway regulates autophagy via regulating Beclin 1, J. Biol. Chem. 284 (2009) 21412–21424.
[39] Y. Kabeya, N. Mizushima, T. Ueno, A. Yamamoto, T. Kirisako, et al., LC3, a mammalian homologue of yeast Apg8p, is localized in autophagosome membranes after processing, EMBO J. 19 (2000) 5720–5728.
[40] P. Matarrese, B. Ascione, L. Ciarlo, R. Vona, C. Leonetti, et al., Cathepsin B inhibition interferes with metastatic potential of human melanoma: an in vitro and in vivo study, Mol. Cancer 9 (2010) 207.
[41] B.C. Victor, A. Anbalagan, M.M. Mohamed, B.F. Sloane, D. Cavallo-Medved, Inhibition of cathepsin B activity attenuates extracellular matrix degradation and inflammatory breast cancer invasion, Breast Cancer Res. 13 (2011) R115.
[42] N.P. Withana, G. Blum, M. Sameni, C. Slaney, A. Anbalagan, et al., Cathepsin B inhibition limits bone metastasis in breast cancer, Cancer Res. 72 (2012) 1199–1209.
[43] C.M. Overall, O. Kleifeld, Tumour microenvironment-opinion: validating matrix metalloproteinases as drug targets and anti-targets for cancer therapy, Nat. Rev. Cancer 6 (2006) 227–239.
[44] M.A. Glozak, N. Sengupta, X. Zhang, E. Seto, Acetylation and deacetylation of non-histone proteins, Gene 363 (2005) 15–23.
[45] Y. Zhang, M. Zhang, H. Dong, S. Yong, X. Li, et al., Deacetylation of cortactin by SIRT1 promotes cell migration, Oncogene 28 (2009) 445–460.
[46] B.J. North, B.L. Marshall, M.T. Borra, J.M. Denu, E. Verdin, The human Sir2 ortholog, SIRT2, is an NAD+-dependent tubulin deacetylase, Mol. Cell 11 (2003) 437–444.
[47] J.P. Dompierre, J.D. Godin, B.C. Charrin, F.P. Cordelieres, S.J. King, et al., Histone deacetylase 6 inhibition compensates for the transport deficit in Huntington's disease by increasing tubulin acetylation, J. Neurosci. 27 (2007) 3571–3583.
[48] J. Lugrin, E. Ciarlo, A. Santos, G. Grandmaison, I. dos Santos, et al., The sirtuin inhibitor cambinol impairs MAPK signaling, inhibits inflammatory and innate immune responses and protects from septic shock, Biochim. Biophys. Acta 1833 (2013) 1498–1510.
[49] G.M. Marshall, P.Y. Liu, S. Gherardi, C.J. Scarlett, A. Bedalov, et al., SIRT1 promotes N-Myc oncogenesis through a positive feedback loop involving the effects of MKP3 and ERK on N-Myc protein stability, PLoS Genet. 7 (2011) e1002135.
[50] S. Nada, A. Hondo, A. Kasai, M. Koike, K. Saito, et al., The novel lipid raft adaptor p18 controls endosome dynamics by anchoring the MEK–ERK pathway to late endosomes, EMBO J. 28 (2009) 477–489.
[51] D.J. Mitchell, K.R. Blasier, E.D. Jeffery, M.W. Ross, A.K. Pullikuth, et al., Trk activation of the ERK1/2 kinase pathway stimulates intermediate chain phosphorylation and recruits cytoplasmic dynein to signaling endosomes for retrograde axonal transport, J. Neurosci. 32 (2012) 15495–15510.
[52] B. Roy, A.K. Pattanaik, J. Das, S.K. Bhutia, B. Behera, et al., Role of PI3K/Akt/mTOR and MEK/ERK pathway in Concanavalin A induced autophagy in HeLa cells, Chemico-Biol. Interact. 210 (2014) 96–102.
[53] S. Cagnol, J.C. Chambard, ERK and cell death: mechanisms of ERK-induced cell death—apoptosis, autophagy and senescence, FEBS J. 277 (2010) 2–21.
[54] A.C. West, R.W. Johnstone, New and emerging HDAC inhibitors for cancer treatment, J. Clin. Investig. 124 (2014) 30–39.